JGR Atmospheres

RESEARCH ARTICLE
10.1029/2020JD032729

Special Section:
Atmospheric PM2.5 in China: physics, chemistry, measurements, and modeling

Gaseous and Particulate Chlorine Emissions From Typical Iron and Steel Industry in China

Xiang Ding[1], Qing Li[1,2], Di Wu[1], Yaoqiang Huo[1], Yingguang Liang[1], Hongli Wang[3], Jie Zhang[4], Shuxiao Wang[5], Tao Wang[6], Xingnan Ye[1,2], and Jianmin Chen[1,2,7]

[1]Shanghai Key Laboratory of Atmospheric Particle Pollution and Prevention, Department of Environmental Science and Engineering, Fudan University, Shanghai, China, [2]Shanghai Institute of Eco-Chongming (SIEC), Shanghai, China, [3]State Environmental Protection Key Laboratory of Formation and Prevention of Urban Air Pollution Complex, Shanghai Academy of Environmental Sciences, Shanghai, China, [4]Jiangsu Provincial Academy of Environmental Science, Nanjing, China, [5]State Key Joint Laboratory of Environmental Simulation and Pollution Control, School of Environment, Tsinghua University, Beijing, China, [6]Department of Civil and Environmental Engineering, Hong Kong Polytechnic University, Hong Kong, China, [7]Center for Excellence in Regional Atmospheric Environment, Institute of Urban Environment, Chinese Academy of Sciences, Xiamen, China

Abstract The accurate estimation of chlorine emissions is urgently needed to evaluate regional and global atmospheric chlorination. This study first reports on the gaseous/particulate phases of chlorine emissions from typical integrated steel industries, including the major manufacturing processes (i.e., sintering, ironmaking, and steelmaking) and self-owned coal-fired power plant (CFPP). The concentration of chlorine species emitted from the ironmaking/steelmaking processes and the self-owned CFPP is very low (<1 mg/Nm^3). Owing to the combustion of chlorine-rich sinter raw materials, the sintering processes emitted unexpectedly high concentrations of chlorinated substances, including chlorinated very short-lived CH_3Cl, CH_2Cl_2, C_2H_5Cl, and $C_2H_4Cl_2$. Flue gas desulfurization (FGD) systems equipped on the sintering processes can slightly reduce chlorinated hydrocarbons emissions (Cl_{VOCs}). However, the chlorine species bonded in filterable/condensable particulate states (Cl_{FPM}/Cl_{CPM}) can be removed by high efficient systems (with efficiencies of 64.8–94.1% for Cl_{FPM} and 97.3–98.5% for Cl_{CPM}), relying on employed FGD technology. Owing to rapid rate at which FGD systems have been installed in China, $Cl_{Inorganic\ gases}$, Cl_{CPM}, and Cl_{FPM} emissions from the sintering and iron industry in 2016 were reduced by 75.3%, 82.7%, and 45.6%, respectively. Our results indicate that the current ultralow-emission equipment facilitates the reduction in chlorine emissions from iron and steel industry, but subsequent retrofits should give greater consideration to the simultaneous removal of Cl_{VOCs}.

Plain Language Summary A significant fraction of tropospheric chlorine atoms, inferred from midcontinental reactive nitrogen chemistry, may arise directly from anthropogenic pollutants. Particulate and gaseous chlorines, as important precursors of chlorine atoms, are mainly derived from anthropogenic combustion sources in polluted inland areas. The characteristics of chlorine emission from combustion sources in China mainly focus on coal and biomass combustion, most of which investigated the chlorine content in coal, raw materials, and by-products according to mass conservation of chlorine; however, there are still very few field-based studies on the chlorine emissions from industrial processes. Therefore, a full-scale field study of chlorine emissions was conducted at typical iron and steel industrial processes in China including steel sintering, ironmaking, steelmaking, and self-owned coal-fired power plant. Owing to the combustion of chlorine-rich raw materials, the steel and iron industry has emitted unexpectedly high concentrations of chlorinated substances. Flue gas samples (Cl_{FPM}, Cl_{CPM}, $Cl_{Inorganic\ gases}$, and Cl_{VOCs}) were collected from the inlets and outlets of the existing FGD systems to investigate their effects on speciation and distribution of the sintering flue gas, providing a scientific basis for the control and supervision of chlorine emission in the steel industry.

Key Points:
- Sintering is identified to be an important emission source of chlorine species in filterable/condensable particulate and gaseous states
- Unexpected high concentrations of chlorinated very short-lived CH_3Cl, CH_2Cl_2, C_2H_5Cl, $C_2H_4Cl_2$, and C_2H_3Cl are emitted from the sintering processes
- Removal efficiency, relying on FGD technology, is much higher for chlorine species contained in particles than that in gaseous states

Supporting Information:
- Supporting Information S1

Correspondence to:
Q. Li,
qli@fudan.edu.cn

Citation:
Ding, X., Li, Q., Wu, D., Huo, Y., Liang, Y., & Wang, H., et al. (2020). Gaseous and particulate chlorine emissions from typical iron and steel industry in China. *Journal of Geophysical Research: Atmospheres*, *125*, e2020JD032729. https://doi.org/10.1029/2020JD032729

Received 11 MAR 2020
Accepted 20 JUL 2020
Accepted article online 25 JUL 2020

1. Introduction

Chlorine atoms (Cl•) are well known to affect the atmospheric lifetimes of volatile organic compounds (VOCs), nitrogen oxides (NO_x), ozone (O_3), and mercury (Saiz-Lopez & Glasow, 2012; Simpson et al., 2015). Some reactive chlorine species are oxidizing agents in the troposphere, such as chlorine (Cl_2), hypochlorite

(HOCl), and nitrochloride ($ClNO_2$), and are easily photolyzed into highly reactive Cl•, resulting in the acceleration of VOC oxidation and ultimately increasing the formation of O_3, organic peroxyl radicals (RO_2•), and cycling of hydroxyl (OH•), and hydroperoxyl radicals (HO_2•) (Qiu, Ying, Wang, Duan, Wang, et al., 2019; Tan et al., 2017). High concentrations of tropospheric chlorine atoms have been reported in coastal cities and urban areas, as well as in polar regions (Liao et al., 2014; Liu et al., 2017). However, a larger atomic chlorine source has also been identified, which can participate in the reactive nitrogen chemistry at nighttime in inland area (Thornton et al., 2010). The chloride-containing aerosols (particulate Cl), which constitute the major fraction of particulate matter (PM), have also been documented to indirectly increase troposphereic oxidation through the conversion to the Cl• precursor-$ClNO_2$ via a nighttime heterogeneous reaction with nitrogen pentoxide (N_2O_5). Some gaseous HCl generated by Cl• that reacts with VOCs almost always provides a larger reservoir to above process through equilibrium repartitioning to particulate Cl^-. Particulate Cl^- and gaseous HCl have also played important roles in a comprehensive assessment for chorine initiated reactions in tropospheric chemistry. The effect of atomic chlorine formation on air quality is not only limited to the coastline, it also spreads much further inland. The sources of uncertainties of particulate Cl^- and gaseous HCl impede the accurate assessment of the regional and global impacts of the above processes. The ocean is the dominant natural source of chlorine emissions on a global scale, contributing nearly 80% of gaseous HCl and particulate Cl^- in the form of sea salt (Erickson et al., 1999; Keene et al., 1999). The contribution of anthropogenic emissions that primarily originate from combustion processes has been reported to be relatively small (McCulloch et al., 1999). However, their regional and local impacts on inland cities cannot be ignored.

The anthropogenic emissions of HCl and particulate Cl^- in 2014 in China were estimated to be 458 and 486 Gg, respectively, and were primarily concentrated in North and Northeast China (Fu et al., 2018). The frequent occurrence of haze accompanied by strong photochemical reactions in these two areas may be related to the high concentrations of inorganic chlorine emissions (Qiu, Ying, Wang, Duan, Wang, et al., 2019; Qiu, Ying, Wang, Duan, Zhao, et al., 2019; Tan et al., 2017; Tham et al., 2016). Coal consumption increased fourfold from 1990 to 2014 in China, but the level of inorganic chloride emissions decreased by ~75% due to widely installed air pollution control devices (APCDs) (Fu et al., 2018; McCulloch et al., 1999). This decreasing trendency has also been documented in other developed countries including the United States, since strict emission standards have been executed for industrial coal combustion to reduce PM and SO_2 emissions (Lee et al., 2018). The relative contribution of inorganic chloride emissions from industrial coal combustion to the total anthropogenic emissions has decreased in China since the introduction of the ultralow-emission standards policy in 2014 (Fu et al., 2018; Tang et al., 2019).

The iron and steel industries, including sintering, ironmaking, and steelmaking processes, are major industries in China that consume about 40% of the world's iron ore (Wang et al., 2018) and account for approximately 58% of the total fine particulate Cl^- emissions from all industrial processes in China (Fu et al., 2018). The relatively higher Cl^- fraction in $PM_{2.5}$ (fine PM with a diameter of 2.5 μm or less) is attributed to the combined combustion of coal, chlorine-rich sinter raw materials, and $CaCl_2$-rich auxiliary materials (Hleis et al., 2013). Electrostatic precipitators (ESPs) are commonly installed in the stacks of ironmaking and steelmaking plants to control dust emissions. Dedusting and flue gas desulfurization (FGD) systems have also typically been installed as an end-pipe technology to allow the complex sintering flue gas to meet the recent low-emission requirements. Various FGD technologies have been developed for sintering flue gases, including wet FGD (such as limestone/ammonia wet FGD), semidry FGD (such as circulating fluidized bed-FGD), and dry FGD (such as activated coke FGD) technologies. The chemical composition of $PM_{2.5}$ at the stack exit depends on the FGD technologies and desulfurizers employed (Ding et al., 2019). Chlorine-rich materials coburn incompletely with fuel and possibly release high concentrations of organic/inorganic chlorine to the flue gases.

There is still no systematic estimation for organic/inorganic chlorine emissions from industrial processes and the effect of commonly used APCDs on the chlorine emissions in particulate and/or gaseous states. We conducted a field study on the chlorine emissions in typical steel plants. To reveal the emission and transformation characteristics of the chlorine in the integrated iron and steel processes, the chlorine in filterable/condensable particulate states (Cl_{FPM}/Cl_{CPM}) and gaseous states released from the three main manufacturing processes (i.e., sintering, ironmaking, and steelmaking) and self-owned coal-fired power

plant (CFPP) were systematically investigated in this study. Self-owned CFPPs were commonly equipped in large-scale steel plants in China to recycle the surplus blast furnace gas for power generation and reduce the cost of electricity for enterprises. Thus, the emissions of a self-owned CFPP in the studied steel plant are also included in this study. The effects of FGD systems (including limestone/ammonia wet FGD and activated carbon dry FGD) installed in the sintering process were evaluated to reveal the chlorine distribution in gaseous/particulate states and organic/inorganic states. An up-to-date emission inventory of the gaseous/particulate and organic/inorganic chlorine based on the diversity of sintering FGD systems is provided and discussed for the period from 2005–2016.

2. Materials and Methods

2.1. Sampling Units

Three typical iron and steel enterprises, all located in North China and with an annual production of approximately 10×10^6 t of steel, were selected for this study. Except the steel rolling process (which produces unorganized emissions, i.e., emissions directly leaked into the atmosphere without an installed sealing equipment), emissions from most of the traditional iron and steel production processes were measured and estimated in the field. The desulfurization and dust removal facilities typically used wet/dry FGD, ESPs, and bag filters, whereas wet ESPs (WESP) were employed following wet FGD (WFGD) to further remove dusts and slurries, as detailed in our previous study (Ding et al., 2019). The three tested sintering processes (labeled as 1#, 2#, and 3#) employed limestone or ammonia WFGDs combined with WESPs and activated coke dry FGD, respectively. The areas of the three tested sintering machines were 180×2, 360, and 600 m^2, respectively. The sampling sites were located at the FGD inlets and the stacks of the three sintering machines (also called the FGD outlets), whereas the sampling sites for ironmaking, steelmaking, and self-owned CFPP were located at the emission stacks. Detailed information on the sampling sites and plants is shown in Figure 1 and supporting information Table S1.

2.2. Sampling Equipment and Method

The sampling of filterable PM (FPM), condensable PM (CPM), and $Cl_{Inorganic\ gases}$ (including gaseous HCl and other inorganic chlorine-containing gases) was performed with an ESC C-5000 isokinetic sampling system (Environmental Supply Company, USA) according to USEPA Methods 201A, 202, and 26A, respectively. Figure S1 shows a schematic of the sampling process, which consisted of an FPM direct-sampling system, a CPM condensate collection system, and a gaseous HCl alkali absorption system in series. The isokinetic nozzle, FPM filter holder, and sampling probe were all heated to 120°C to avoid the condensation of gases on walls of the sampling tubes. The FPM was collected on Teflon filters (Whatman 7592-104, UK) for further analysis. The residual FPMs on the filter holders were rinsed twice with acetone and collected in the blue-capped bottles for weighing after evaporation. The CPM was primarily collected in an ultrapurewater dropout and dry impingers, which were soaked in a water bath (<30°C). To improve the collection efficiency of CPM, a CPM filter holder was installed after the water dropout and dry impingers. The $Cl_{Inorganic\ gases}$ (the remaining gases after condensation) was always discharged into the atmosphere in a gaseous state and collected in two-stage impingers containing 50 ml of 30 mmol/L NaOH solutions after the CPM filter in this study. The CPM collection trains were immediately purged with high-purity N_2 (≥99.9%, flow rate of 15 L/min) for 90 min to remove soluble gases ($Cl_{Inorganic\ gases}$, SO_2, and NO_2) to the $Cl_{Inorganic\ gases}$ absorption liquid after sampling. Ultrapure water and organic solvent (acetone and hexane) were then used to rinse each part before the CPM filter holders twice in sequence, as detailed in our previous study (Liang et al., 2020).

The sampling times for FPM, CPM, and inorganic gaseous Cl samples were all set to 30 min. Additionally, VOC samples were collected in polyvinyl fluoride (PVF) bags by a portable vacuum gas sampler with a flow rate of 1 L/min and analyzed within 8 hr. Other gaseous pollutants, including CO, NO, NO_2, SO_2, and CH_4, were monitored using a flue gas analyzer (Testo 370, Germany). Three successful samples of the above pollutants were collected in parallel at each sampling site.

2.3. Chemical Analysis and Quality Control

The leakage check and the sampling flow rate calibration were performed before each PM and gaseous pollutant sampling. The FPM and CPM Teflon filters were weighed on an analytical balance (Sartorius,

Figure 1. (a) Location of the sampling sites in the tested iron and steel plants; (b) sintering process: (I) the head of sintering machine (sinter head), (II) the tail of sintering machine (sinter tail), (III) lime-gypsum wet flue gas desulfurization (L-WFGD), (IV) ammonia wet flue gas desulfurization (A-WFGD), and (V) activated coke dry flue gas desulfurization (AC-FGD); (c) ironmaking process: (I) the blast furnace and (II) electrostatic precipitator + fabric filter (ESP + FF); (d) steelmaking process: (I) the converter and (II) ESP + FF; and (e) self-owned CFPP: (I) selective catalytic reduction (SCR), (II) ESP, and (III) L-WFGD.

MSE6.6S-0CE-DM, Germany) in a constant-temperature humidity chamber (50% RH and 20°C). One-quarter of each filter was used to analyze the water-soluble ions. The filters were extracted with 10 ml ultrapure water for 30 min. The Cl^- and other ions were examined on an ion chromatograph (940 Professional IC, Metrohm, Switzerland) with detection limits between 0.47 and 3.33 ng/ml; a separation column (Metrosep A Supp 16-250, Metrohm) and a guard column (Metrosep C6, Metrohm) were used to separate Cl^- from the other ions. The Cl^- in the field-collected gaseous HCl and CPM solution samples was also analyzed using ion chromatography. All forms of Cl in the particles (Cl^- and insoluble Cl in water) were detected. The remaining three quarters of each filter was placed in a digestion vessel, and a mixture of 4 ml HNO_3 (30%) and 1 ml H_2O_2 was added to digest the sample at 170°C for 4 hr. The solutions were diluted to 10 ml with ultrapure water after cooling. The concentrations of elemental Cl and other elements were determined via inductively coupled plasma mass spectrometry (ICP-MS 7500a, Thermo, USA).

PVF bags were cleaned with dehydrocarbon air at least three times before VOC sampling. Speciated VOCs were analyzed using gas chromatography/mass spectrometry (GC/MS). The GC/MS system consisted of a preconcentrator (Entech 7200, USA), an autosampler (Entech 7032AB), a gas chromatograph (Agilent 7890B GC System, USA), and a mass selective detector (Agilent 5977B GC/MSD, USA). The VOC analysis was performed for PAMS and TO-15 target VOCs. A DB-5ms GC column (Agilent Technologies, dimensions 60 m × 0.25 mm × 1.00 μm, USA) was used for the separation of chlorinated VOC species. The retention times and mass spectra were used for the identification of VOC species. Each collected VOC sample bag was analyzed in parallel for quality assurance.

2.4. Bottom-Up Inventory Calculation

The gaseous and particulate chlorine emission factors (EFs) were determined based on the parameters of flue gases listed in Table S1 for the sinter, ironmaking, and steelmaking. EFs for each process can be calculated with the following equation:

$$EF_{i,j} = C_{i,j} \cdot Q_j \cdot P_j^{-1} \cdot 10^{-3}$$

where i indicates the type of chloride pollutant, including Cl_{FPM}, Cl_{CPM}, $Cl_{Inorganic\ gases}$, and Cl_{VOCs}; j indicates different production processes, covering the sintering, ironmaking, and steelmaking; $EF_{i,j}$ is the pollutant i EF from production process j (g/t); $C_{i,j}$ is the average emitted mass concentration of pollutant i from production process j at normal condition (101.325 kPa, 273.15 K) with the unit of mg/Nm^3; Q_j is the flue gas volume flow in production process j (Nm^3/hr); and P_j is the average amount of product per unit time with the unit of t/hr.

FGDs as SO_2 abatement technologies have been rapidly installed in steel sintering processes in recent years; however, the annual variation of FGDs application rate was not included for the estimating the gaseous and particulate chlorine emissions in previous studies (Fu et al., 2018; McCulloch et al., 1999). To better understand annual variation in the steel sintering chlorine emissions during the period of 2005–2016, FGD technology-based method was applied to estimate the emissions of Cl_{FPM}, Cl_{CPM}, $Cl_{Inorganic\ gases}$, and Cl_{VOCs} in this study. The annual chlorine emission from the steel sintering industry was calculated with the following equation:

$$E_{i,c} = \sum_{i,p} EF_{i,p} \cdot A_{p,c}$$

where c is the calendar year; $E_{i,c}$ is annual atmospheric emissions of pollutant i in calendar year c (t/yr); p is the type of FGD technology, including limestone or ammonia WFGD, semidry FGD, activated coke dry FGD, and non-FGD (the flue gas after ESP process discharged directly without downstream FGD system treatment); $EF_{i,p}$ is the average EF of pollutant i for sintering after FGD process p (g/t); and $A_{p,c}$ is the activity level of sintering after FGD process p in calendar year c. A refined activity database about sintering desulfurization facilities listed by MEP is established, including sintering FGD commissioning date and installed capacity (MEP, 2014, 2016; Wang et al., 2019); detailed information on the activity level of sintering after wet/semidry/dry FGD process is listed in Table S2. The historical production outputs of sinter ore from 2005 to 2016 are obtained from the China Steel Yearbook (CISIA, 2001–2016; Wu et al., 2017).

3. Results and Discussion

3.1. Distribution of Inorganic Cl in Gaseous and Particulate Phases

Figure 2 shows the mass distribution of inorganic Cl among the three parts, that is, the FPM filter holder (Cl_{FPM}), the dry impingers and CPM filter holder (Cl_{CPM}), and the alkali absorption liquids ($Cl_{Inorganic\ gases}$) of the inorganic Cl sampling system, collected from the different processes of typical steel plants. The average total inorganic chlorine concentrations in the flue gases from stacks of the sintering, ironmaking, steelmaking, and self-owned CFPP were 3.55 ± 3.11, 0.94 ± 0.61, 0.55 ± 0.17, and 0.85 ± 0.36 mg/Nm^3, respectively. The highest concentration of inorganic chlorines emissions occurred in the sintering processes, likely due to the combustion of raw materials containing high level of chlorine in this process. Although the dedusters were installed after each process to remove particulate emissions, the Cl_{FPM} in the stack flue gas still dominates the total inorganic Cl emission, with Cl_{FPM} content varying from 57.6% to 99.1%. As shown in Figure 2, there were almost no $Cl_{Inorganic\ gases}$ or Cl_{CPM} emissions from the ironmaking and steelmaking processes. This phenomenon is consistent with the near-zero emissions of SO_2 and NO_x (see Table S1). The $Cl_{Inorganic\ gases}$ and Cl_{CPM} emissions in the steel industry are primarily released during the sintering process. According to EPA Methods 201A and 202, Cl_{CPM} is generated in the cooling tubes from gas-phase precursors (i.e., HCl), whose concentrations depend on the APCDs and other specific conditions including combustion and flue gas temperatures (Yang et al., 2015). The three tested FGD systems all effectively controlled Cl_{CPM} and $Cl_{Inorganic\ gases}$ emissions. The activated coke FGD can directly remove $Cl_{Inorganic\ gases}$ due to its own adsorption characteristics, whereas $Cl_{Inorganic\ gases}$ can be absorbed by the aqueous phase of the absorbent

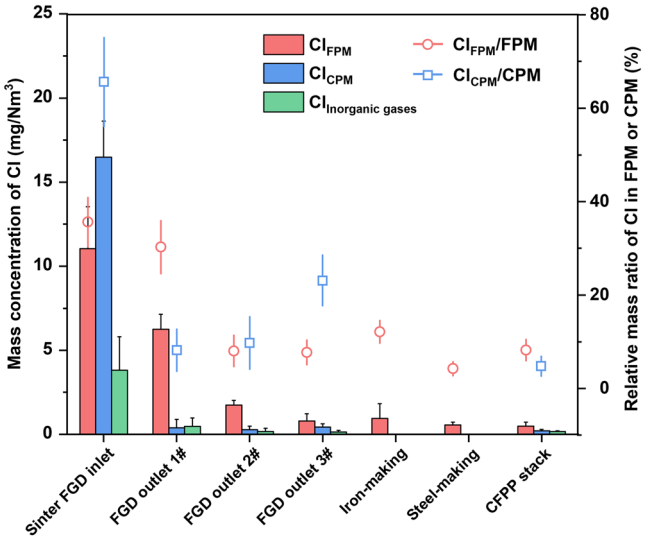

Figure 2. Mass concentrations of inorganic chlorines in inorganic gaseous ($Cl_{Inorganic\ gas}$) and particulate states (Cl_{FPM} and Cl_{CPM}) emitted from different processes in typical iron and steel plants, as well as their relative mass ratios in FPM (Cl_{FPM}/FPM) and CPM (Cl_{FPM}/CPM). FGD Outlets 1#, 2#, and 3# labeled on the figure denote the sintering stacks after limestone WFGD, ammonia WFGD, and activated coke dry FGD processes, respectively.

slurry in the WFGD systems and then dissociated to form Cl^-: $HCl_{(g)} \leftrightarrow HCl_{(aq)} \leftrightarrow H^+_{(aq)} + Cl^-_{(aq)}$ (Córdoba, 2015). The $Cl_{Inorganic\ gases}$ and Cl_{CPM} concentrations at the two FGD outlets for the sintering process decreased by 87.7–96.6% and 97.4–98.3%, respectively.

Both Cl_{FPM} and Cl_{CPM} can contribute to the chlorine in PM (i.e., $Cl_{PM} = Cl_{FPM} + Cl_{CPM}$) after the flue gas is released into the atmosphere. The significant difference in the removal efficiencies of Cl_{FPM} among the different FGD systems is primarily caused by their removal mechanisms in the dry/wet FGD systems, as detailed in our previous study (Ding et al., 2019). Cl_{FPM} was removed with an efficiency of up to 92.8 ± 2.1% by the activated coke FGD through adsorption and filtration, whereas the limestone and ammonia WFGD processes can convert $Cl_{Inorganic\ gases}$ into particulate Cl via heterogeneous condensation with in the desulfurization slurries. $Cl_{Inorganic\ gases}$ and Cl_{PM} can achieve a thermodynamic equilibrium, which results in an increase of the particle acidity of flue gases (Lee et al., 2018). Thus the proportion of Cl in FPM at ammonia WFGD outlet is lower than that at the limestone WFGD outlet (see Figure 2). These concentrations and ratios at the FGD outlets reveal that FGD type determines the mass distribution of inorganic Cl in sintering stacks as a result of their diverse removal mechanisms.

3.2. Organic Chlorine Emissions

Chlorinated hydrocarbons emissions (Cl_{VOCs}) are another important emission form of organic Cl in iron and steel processes. Figure S3 shows the emission profiles of 117 tested nonmethane hydrocarbons (NMHCs) based on carbon number. The Cl_{VOCs} mass fractions of the total NMHCs were 16.9 ± 7.6%, 13.3 ± 3.7%, 19.5 ± 3.4%, and 7.1 ± 2.2% for sintering, ironmaking, steelmaking, and self-owned CFPP, respectively. The high concentrations of Cl_{VOCs} associated with the sintering process may be attributable to incomplete combustion of chlorinated fuel and raw coal. The Cl_{VOCs} are dominated by C_1-C_2 compounds, which represent with ranging from 94.5% to 97.1% of the Cl_{VOCs}. The Cl_{VOCs} with C_1-C_2 are also called chlorinated very short-lived substances (Cl_{VSLS}), which are significant sources of the stratospheric chlorines that contribute to ozone depletion (Claxton et al., 2019; Hossaini et al., 2017, 2019). The compounds dichloromethane (CH_2Cl_2) and chloroform ($CHCl_3$), accounting for ~90% and ~25% of their tropospheric abundance from anthropogenic activities (Hossaini et al., 2015), respectively, are the relatively abundant Cl_{VSLS} produced by the sintering process.

Figure 3 details the concentrations of various Cl_{VSLS} directly emitted by the different tested processes in the iron and steel industries. The total concentration of emitted Cl_{VSLS} was the highest for the sintering stacks (FGD Outlets 1#, 2#, and 3#) with an average value of 401 ± 164 ppb Cl followed by that from ironmaking (23.3 ± 4.2 ppb Cl), self-owned CFPP (23.0 ± 7.1 ppb Cl), and steelmaking (15.2 ± 3.8 ppb Cl). For the sintering stacks, methyl chloride (CH_3Cl) was the major Cl_{VSLS} species with average concentration of 352 ± 31 ppb Cl. The concentrations of dichloromethane (CH_2Cl_2), chloroethane (C_2H_5Cl), 1,2-dichloroethane ($C_2H_4Cl_2$), and vinyl chloride (C_2H_3Cl) were also greater than 10 ppb Cl. The chloro-substituted reaction during combustion primarily involved the dominant VOCs species (i.e., CH_4, C_2H_6, and C_2H_4), as shown in Figure S2 and Table S1. Owing to the high volatility and stability of the above Cl_{VSLS}, the removal efficiencies of these substances in the FGD systems are very low and are much lower than those inorganic Cl compounds. Among these Cl_{VSLS}, CH_2Cl_2 is known to be emitted primarily from solvent/feedstock for paint removal and foam/hydrofluorocarbon production (Feng et al., 2018; Simmonds et al., 2006), whereas $CHCl_3$ is primarily emitted from hydrofluorocarbon manufacturing and is a by-product of the water chlorination and bleaching processes (Rhew et al., 2008). Although the Cl_{VSLS} concentrations from the iron and steel plants are not significant in comparison with other common pollutants such as SO_2 and NO_x, their emission of certain ozone-depleting compounds cannot be ignored and has the great potential to influence future ozone projections as their atmospheric lifetimes are approximately 6 months (Keene et al., 1999).

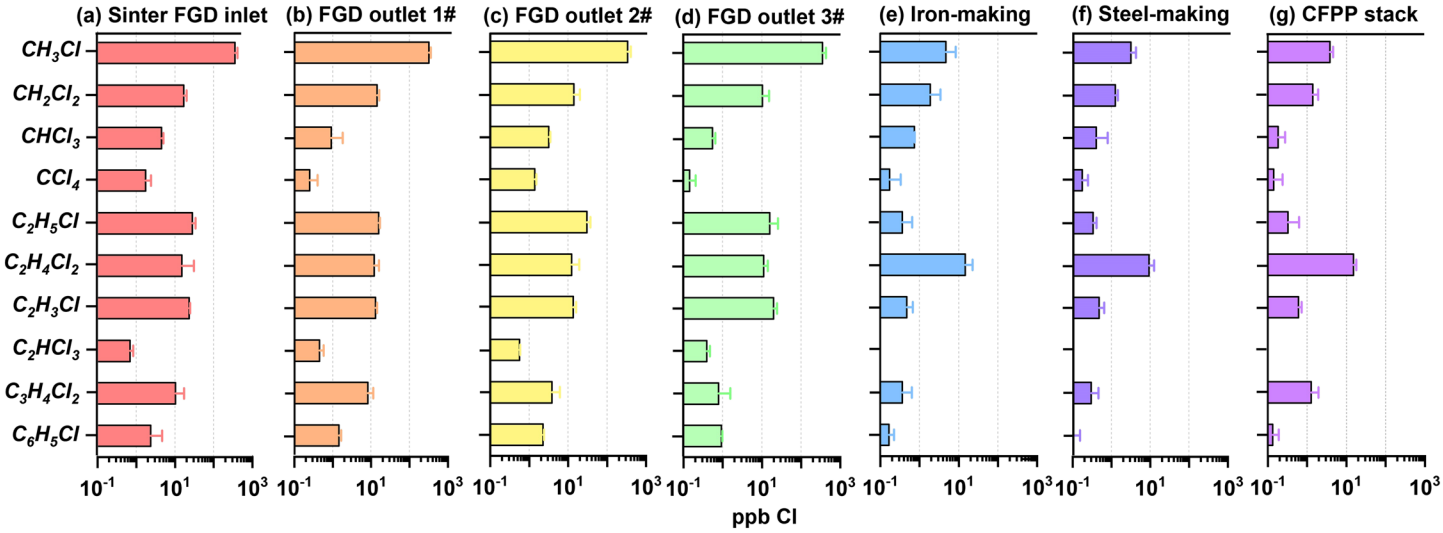

Figure 3. Concentrations of chlorinated very short-lived substances (CH_3Cl, CH_2Cl_2, $CHCl_3$, CCl_4, C_2H_5Cl, $C_2H_4Cl_2$, C_2H_3Cl, and C_2HCl_3) and other major chlorinated VOC species ($C_3H_4Cl_2$ and C_6H_5Cl) emitted from different processes at typical iron and steel plants. Samples were obtained from (a) the inlet of the sintering FGD installed in the downstream of the ESP; the sintering FGD outlets (b) 1#, (c) 2#, and (d) 3#; (e) the ironmaking stack; (f) the steelmaking stack; and (g) the self-owned CFPP stack.

Figure S3 summarizes the relative proportions of chlorinated hydrocarbons in the total NMHC emissions including the major reported anthropogenic emissions (He et al., 2015; Mo et al., 2015; Shen et al., 2018; Shi et al., 2015; Tsai et al., 2008; Wang et al., 2013; Wei et al., 2008; Zheng et al., 2013). This comparison of the Cl_{VOCs} relative abundance shows that the chlorinated hydrocarbon emissions from industrial processes are higher than those from other anthropogenic sources. With the exception of chlorinated industry emissions, the iron and steel industries have the highest abundance of Cl_{VOCs}. This finding suggests that we must pay more attention to the emissions of Cl_{VOCs} from the iron and steel industries.

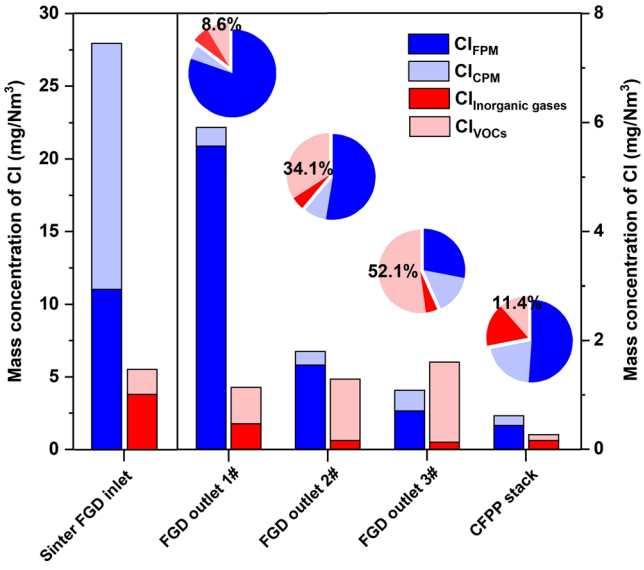

Figure 4. Emission concentrations and mass distribution of major tropospheric Cl species bonded in filterable/condensable particulate phases and volatile organic/inorganic gaseous phases during the processes of sintering and self-owned CFPP. FGD Outlets 1#, 2#, and 3# denote the samples obtained in the sintering stacks after limestone, ammonia, and activated coke FGD process, respectively.

3.3. Distribution of Chlorinated Compounds

Figure 4 shows the mass concentrations of chlorine emissions and their relative distribution in various states obtained from the tested sintering processese quipped with various FGD systems and the self-owned CFPP equipped with the limestone WFGD system. The mass concentration of total chlorine at the sintering FGD inlet is 32.61 ± 5.44 mg/Nm^3. After the flue gases pass through the sintering FGD process, the total chlorine mass concentration was 8.21 ± 2.47 mg/Nm^3 at the limestone WFGD outlet and was much lower at the ammonia WFGD and the activated coke FGD outlets with values ranging from 2.45–3.34 mg/Nm^3. The higher Cl concentrations generated in the sintering process can be attributed to the high chlorine content of the raw materials. The total chlorine concentration at the FGD inlet of the self-owned CFPP (11.1 ± 3.1 mg/Nm^3) is much lower than that at the FGD inlet of the sintering processes. The mass concentrations at the sintering stacks equipped with the limestone WFGD system were nearly 9 times higher than those (0.96 ± 0.15 mg/Nm^3) at the self-owned CFPP stacks equipped with the same FGD system. The removal efficiency of total chlorine from self-owned CFPP with ultralow emission is clearly higher than that of the sintering industry.

Table 1
Average Emission Factors of Cl_{FPM}, Cl_{CPM}, $Cl_{Inorganic\ gases}$, Cl_{VOCs}, and Cl_{VSLS} Obtained From Sintering, Ironmaking, Steelmaking Process (in g Cl/t Product) and Self-Owned CFPP (in g Cl/t Coal)

	Iron and steel industry							
	Sintering (g Cl/t sinter ore)					Ironmaking (g Cl/t pig iron)	Steelmaking (g Cl/t crude steel)	Self-owned CFPP (g Cl/t coal)
	After APCDs							
	ESP (non-FGD)	ESP + L-WFGD	ESP + A-WFGD	ESP + AC-FGD	ESP + CFB-FGD	ESP + FF	ESP + FF	SCR + ESP + L-WFGD
Cl_{FPM}	25.05 ± 5.65	14.20 ± 2.02	4.39 ± 0.71	1.65 ± 0.90	0.3 ± 0.1[a]	0.55 ± 0.52	0.52 ± 0.16	3.92 ± 1.84
Cl_{CPM}	37.41 ± 4.87	0.88 ± 1.13	0.71 ± 0.50	0.90 ± 0.42		0.01 ± 0.01	0.01 ± 0.01	1.60 ± 0.72
$Cl_{Inorganic\ gases}$	8.64 ± 4.56	1.07 ± 1.23	0.40 ± 0.53	0.27 ± 0.21		0.02 ± 0.02	0.01 ± 0.01	1.28 ± 0.32
Cl_{VOCs}	2.90 ± 0.66	2.43 ± 0.41	2.93 ± 0.66	2.29 ± 0.50		0.10 ± 0.03	0.08 ± 0.03	`0.88 ± 0.24
CH_3Cl	1.686 ± 0.290	1.556 ± 0.174	1.755 ± 0.357	1.533 ± 0.357		0.006 ± 0.005	0.007 ± 0.002	0.070 ± 0.014
CH_2Cl_2	0.137 ± 0.026	0.116 ± 0.016	0.124 ± 0.052	0.074 ± 0.035		0.004 ± 0.003	0.005 ± 0.001	0.043 ± 0.016
$CHCl_3$	0.051 ± 0.005	0.01 ± 0.01	0.039 ± 0.005	0.006 ± 0.001		0.002 ± 0.001	0.002 ± 0.002	0.008 ± 0.004
CCl_4	0.026 ± 0.01	0.004 ± 0.002	0.022 ± 0.002	0.002 ± 0.001		0.001 ± 0.001	0.001 ± 0.001	0.008 ± 0.005
C_2H_5Cl	0.173 ± 0.036	0.096 ± 0.008	0.201 ± 0.047	0.087 ± 0.056		0.001 ± 0.001	0.001 ± 00.001	0.008 ± 0.007
$C_2H_4Cl_2$	0.142 ± 0.149	0.114 ± 0.038	0.125 ± 0.073	0.095 ± 0.026		0.038 ± 0.020	0.038 ± 0.014	0.544 ± 0.103
C_2H_3Cl	0.139 ± 0.008	0.077 ± 0.008	0.088 ± 0.016	0.106 ± 0.024		0.001 ± 0.001	0.001 ± 0.001	0.014 ± 0.003
C_2HCl_3	0.009 ± 0.002	0.006 ± 0.002	0.008 ± 0.002	0.004 ± 0.001		<0.001	<0.001	0.003 ± 0.002

Note. APCDs = air pollution control devices; ESP = electrostatic precipitator; L-WFGD or A-WFGD = lime-gypsum or ammonia wet flue gas desulfurization combined with wet electrostatic precipitator; AC-FGD = activated coke dry flue gas desulfurization; CFB-FGD = circulating fluidized bed semidry flue gas desulfurization combined with fabric filter (FF); SCR = selective catalytic reduction.
[a]Reported by Ding et al. (2019).

A comprehensive analysis of the chlorinated components is shown for the organic/inorganic states. The FGD system had no significant effect on the removal of C_{1-2}-based Cl_{VOCs} in the tested sintering processes. The removal efficiencies for the Cl_{VOCs} fraction by the FGD systems were all less than ~17%. The relative contribution of Cl_{VOCs} in total Cl concentration varies greatly before and after the desulfurization processes. The Cl_{VOCs} fraction increased from 3.9% at the sintering FGD inlet to 13.0%, 34.7%, and 44.9% after the flue gases passed through the limestone WFGD, the ammonia WFGD, and the activated coke FGD systems, respectively. All these FGD systems efficiently removed HCl ($Cl_{Inorganic\ gases}$ + Cl_{CPM}) and Cl_{FPM}. The FGD systems are able to remove HCl via both the absorption of desulfurizer and the condensation conversion of HCl to Cl_{FPM} due to the temperature decrease in the FGD towers. The removal efficiency of HCl (96.9 ± 1.1%) was even higher than that of SO_2 (91.4 ± 2.9%) in the FGD processes. The rank of the average removal efficiency of each chlorinated species in these FGD systems was HCl > Cl_{FPM} > Cl_{VOCs}.

The distribution of chlorinated species in gaseous/particulate phases subsequently changed after the flue gases passed through the sintering process. The average concentrations of gaseous and particulate Cl ($Cl_{Inorganic\ gases\ +\ VOCs}$ and $Cl_{FPM\ +\ CPM}$) at the sintering FGD outlets were 1.36 ± 0.15 and 3.30 ± 2.93 mg/Nm^3, respectively. The FGD systems were more efficient in removing particulate Cl than gaseous Cl, because the Cl_{CPM} was derived from ~81% HCl condensation, which accounts for ~60% of the particulate Cl and was easily removed by the FGD systems. Additionally, the relative contribution of particulate Cl decreased from 84.4% at the sintering FGD inlet to 81.2%, 60.4%, and 49.8% after flue gases had passed through the limestone WFGD, the ammonia WFGD, and the activated coke FGD systems, respectively. These results are consistent with the Cl_{FPM} removal efficiency of each desulfurization system.

3.4. Chlorine Emissions From Steel Sintering in China From 2005–2016

Approximately 76.4–91.5% of the total Cl in the sintering flue gas can be efficiently removed by the different FGD systems, and the chlorine emission state at stack exits was also significantly altered by the FGD processes. EFs can be calculated based on the measured Cl concentrations, daily flue gas volume, and sintering yield of the three typical steel sintering processes. Table 1 lists the average EFs of Cl_{FPM}, Cl_{CPM}, $Cl_{Inorganic\ gases}$, and Cl_{VOCs} at the FGD inlets and outlets from the different FGD systems including values reported

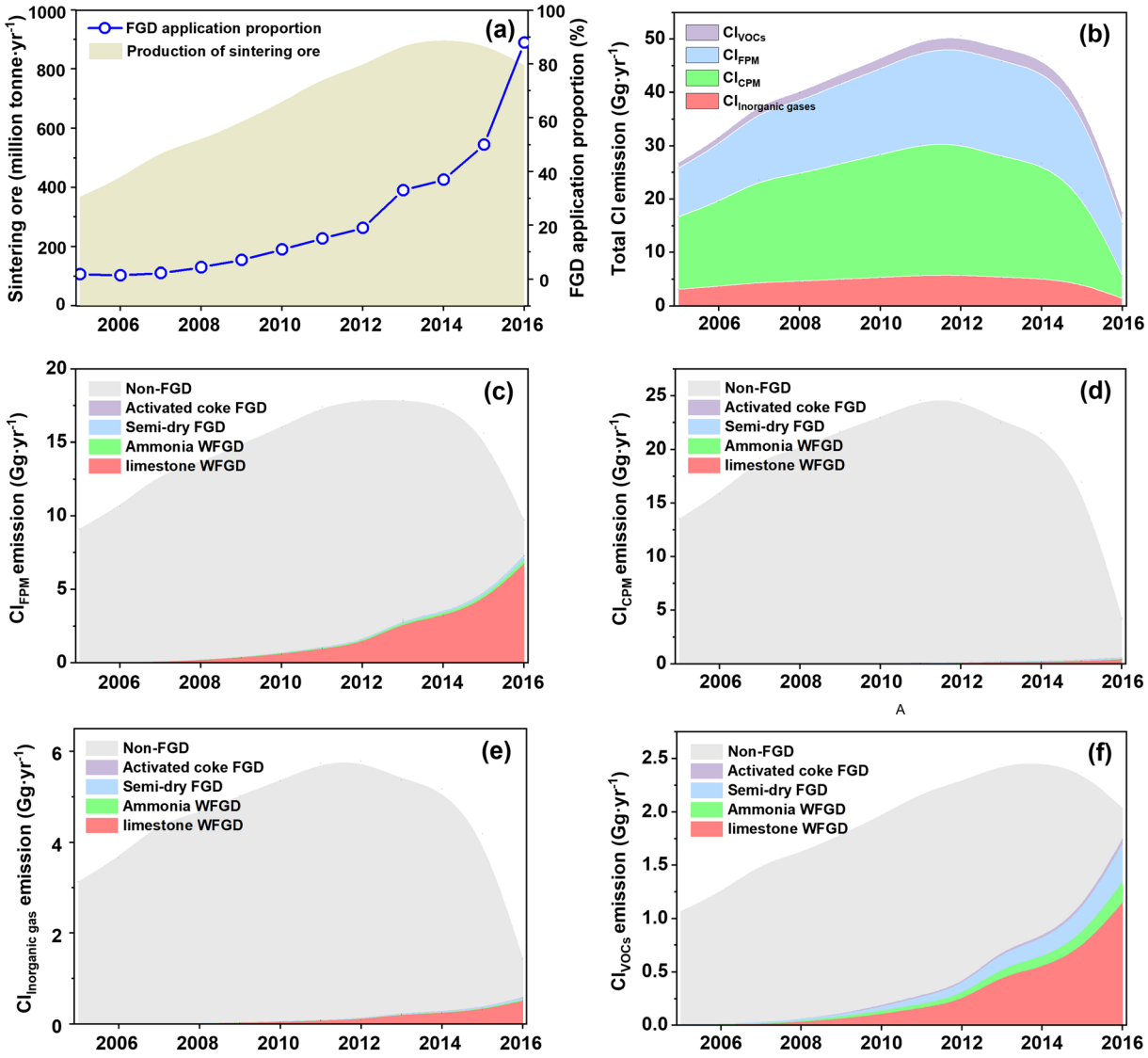

Figure 5. Emission trends for major tropospheric Cl species emitted from sintering in China from 2005–2016. (a) The production of Chinese sinter ore and the installation rate of FGD systems in sintering; (b) total Cl emissions for Cl_{FPM}, Cl_{CPM}, $Cl_{Inorganic\ gases}$, and Cl_{VOCs} estimated from the installation rate, sinter ore production, and pollutant emission factors; and (c) Cl_{FPM}, (d) Cl_{CPM}, (e) $Cl_{Inorganic\ gases}$, and (f) Cl_{VOCs} emissions after the application of different emission abatement technologies (wet/semidry/dry FGD) in sintering. Non-FGD = the flue gas discharged directly without FGD system treatment.

in previous studies. The EF of $Cl_{Inorganic\ gases}$ for the sintering emissions was reported as 0.6 g Cl/(t sinter ore) (Fu et al., 2018), which is within the range of our estimated result of 0.3–1.1 g Cl/(t sinter ore) for the sintering plants equipped with the FGD systems. The EFs of Cl_{FPM} for the sintering equipped with the limestone/ammonia/activated coke FGD systems are higher than for those equipped with a CFB-FGD system, owning to the high dust removal performance of the equipped post-FF (Ding et al., 2019). Among these FGD technologies, the highest EF was exhibited by the Cl_{FPM} from the limestone WFGD system, which is consistent with previous studies (Guo et al., 2017; Jia et al., 2018). No field-measured EFs of Cl_{CPM}, $Cl_{Inorganic\ gases}$, and Cl_{VOCs} emitted by sintering processes after the semidry FGD are available. The similar physical properties including temperature and humidity of sintering flue gases were reported in our previous study (Ding et al., 2019). The EFs of Cl_{CPM}, $Cl_{Inorganic\ gases}$, and Cl_{VOCs} after activated coke FGD were employed to calculate the annual Cl emissions after semidry FGD in this study.

Figure 5 shows the annual total Cl emissions from China's iron and steel industries, preliminarily estimated by including the production of sintering ore and the proportion of plants that had installed FGD systems

from 2005–2016. The total Cl emissions in the steel sintering flue gas are annually updated based on the installation rate of various FGD systems. The installation rate of FGD systems in China was less than 20% until 2012. Before 2012, more than 80% of the sintering flue gas was directly discharged into the atmosphere without treatment by FGD systems, resulting in an increase in the total Cl emission (including Cl_{FPM}, Cl_{CPM}, $Cl_{Inorganic\ gases}$, and Cl_{VOCs}) from 26.9 Gg in 2005 to the peak of 50.7 Gg in 2012 concomitant with the annual increase of steel production. Since 2012, the annual total Cl emissions have gradually decreased as the proportion of FGD systems installed have increased. Owing to strict regulations regarding annual SO_2 emission standards (Wang et al., 2019), the installation rate of wet/semidry/dry FGD systems for steel plants rapidly increased to more than 90% by 2016. The installation of FGD systems leads to decreases in the $Cl_{Inorganic\ gases}$, Cl_{CPM}, and Cl_{FPM} emissions of 75.3%, 82.7%, and 45.6%, respectively.

The FGD systems have played a significant role in controlling inorganic Cl emissions from sintering flue gases in China. The rapid application of the FGD systems has promoted an increase in total Cl removal efficiency, from 1.5% in 2005 to 71.3% in 2016. More than 42 Gg total Cl, which is 2.5 times higher than the actual emitted quantity, was eliminated by the widespread implementation of FGD systems by 2016. More than half of the total Cl emission reduction, which was dominated by particulate phase Cl, was attributable to the efficient removal of Cl_{CPM} by the widely used limestone WFGDs. The relative contribution of Cl_{CPM} continuously dropped from 50.4% in 2005 to 24.5% in 2016, while that of Cl_{FPM} increased from 33.9% in 2005 to 55.7% in 2016. With the rapid installation rate of various FGD systems, Cl_{FPM} will be the major phase of chlorine emitted by the steel industry (see Figures 5b and 5c). Thus, the enhancement of PM removal efficiency to meet ultralow-emission requirements, particularly via the limestone WFGD system, is effective for the synergistic control of the total Cl emissions in the steel industry. However, the Cl_{VOCs} is not effectively eliminated by these tested FGD technologies, as shown in Figure 5f. The relative contribution of Cl_{VOCs} to the total Cl increased from ~3.9% in 2005 to ~11.7% in 2016. The increasing emission level of Cl_{VSLS} could contribute to an increased concentration of tropospheric CH_2Cl_2, which has been reported to have increased from 69 ± 14 ppt Cl in 2000 to 111 ± 22 ppt Cl in 2017 according to long-term surface field measurements (Hossaini et al., 2015, 2017, 2019) and the upper troposphere monitoring data (Leedham Elvidge et al., 2015). Therefore, the Cl_{VOCs} emitted from the sintering process, particularly the Cl_{VSLS}, should be given greater attention in the future with regard to their efficient removal during air pollution control.

4. Conclusions

This study first reports the field-based chloride species emissions in gaseous/particulate phases from the iron and steel industry, one of the significant chlorine-rich raw material combustion sources, mainly including three main manufacturing processes (sintering, ironmaking, steelmaking) and a self-owned CFPP. The average total chlorine concentrations in the flue gases from stacks of the sintering, ironmaking, steelmaking, and self-owned CFPP were 4.67 ± 3.10, 1.14 ± 0.67, 0.74 ± 0.24, and 0.91 ± 0.42 mg/Nm^3, respectively. The sintering process is identified to be an important source of chlorine species in all states. Approximately 76.4–91.5% of the total Cl in the sintering flue gas can be efficiently removed by the different FGD systems, and the chlorine emission state at stack exits was also significantly altered by the FGD processes. The FGD types largely determine the inorganic chlorine mass distribution in sintering stacks, by the difference in the removal effect on inorganic chlorine, including Cl_{FPM}, Cl_{CPM}, and $Cl_{Inorganic\ gases}$. By 2016, the installation rate of emission abatement technology for wet/semidry/dry FGD process had increased rapidly to 90%, leading to decreases of 75.3%, 82.7%, and 45.6% in the average $Cl_{Inorganic\ gases}$, Cl_{CPM}, and Cl_{FPM} emissions, respectively, but no obvious decreases for Cl_{VOCs} emissions. Unexpected high concentrations of very short-lived CH_3Cl, CH_2Cl_2, C_2H_5Cl, $C_2H_4Cl_2$, and C_2H_3Cl are emitted in the sintering processes. Thus, the subsequent ultralow-emission retrofits for APCDs in the iron and steel industry should pay more attention to the synergistic removal of Cl_{VOCs}. The present study mainly updated and provided detailed chlorine EFs and characteristics from typical steel plants. The impact of newly emitted chlorines on tropospheric and stratospheric species is not included in this study and needed further investigation. The extrapolation of the obtained EFs to the whole China is not perfect since the steel plants have their own circumstances. Thus an elaborative inventory is further required with including a detailed local conditions.

Data Availability Statement

The data sets used in this manuscript were available online (https://figshare.com/articles/Data_resulting_from_the_study_for_chlorine_emission_from_typical_Chinese_iron_and_steel_industry/12402860/1).

Acknowledgments
This work was supported by the Ministry of Science and Technology of the People's Republic of China (2018YFC0213800) and the National Natural Science Foundation of China (21876028, 91743202, 21625701, and 91843301). We sincerely appreciate the valuable comments from the reviewers, which greatly helped to improve the quality of our manuscript.

References

CISIA (2001–2016). China steel yearbook (2001–2016), Beijing, China: China Iron and Steel Industry Association (CISIA). (in Chinese)

Claxton, T., Hossaini, R., Wild, O., Chipperfield, M. P., & Wilson, C. (2019). On the regional and seasonal ozone depletion potential of chlorinated very short-lived substances. *Geophysical Research Letters*, *46*, 5489–5498. https://doi.org/10.1029/2018gl081455

Córdoba, P. (2015). Status of Flue Gas Desulphurisation (FGD) systems from coal-fired power plants: Overview of the physic-chemical control processes of wet limestone FGDs. *Fuel*, *144*, 274–286. https://doi.org/10.1016/j.fuel.2014.12.065

Ding, X., Li, Q., Wu, D., Liang, Y., Xu, X., Xie, G., et al. (2019). Unexpectedly increased particle emissions from the steel industry determined by wet/semidry/dry flue gas desulfurization technologies. *Environmental Science & Technology*, *53*(17), 10,361–10,370. https://doi.org/10.1021/acs.est.9b03081

Erickson, D. J., Seuzaret, C., Keene, W. C., & Gong, S. L. (1999). A general circulation model based calculation of HCl and $ClNO_2$ production from sea salt dechlorination: Reactive Chlorine Emissions Inventory. *Journal of Geophysical Research*, *104*(D7), 8347–8372. https://doi.org/10.1029/98jd01384

Feng, Y., Bie, P., Wang, Z., Wang, L., & Zhang, J. (2018). Bottom-up anthropogenic dichloromethane emission estimates from China for the period 2005–2016 and predictions of future emissions. *Atmospheric Environment*, *186*, 241–247. https://doi.org/10.1016/j.atmosenv.2018.05.039

Fu, X., Wang, T., Wang, S., Zhang, L., Cai, S., Xing, J., & Hao, J. (2018). Anthropogenic emissions of hydrogen chloride and fine particulate chloride in China. *Environmental Science & Technology*, *52*(3), 1644–1654. https://doi.org/10.1021/acs.est.7b05030

Guo, Y., Gao, X., Zhu, T., Luo, L., & Zheng, Y. (2017). Chemical profiles of PM emitted from the iron and steel industry in northern China. *Atmospheric Environment*, *150*, 187–197. https://doi.org/10.1016/j.atmosenv.2016.11.055

He, Z., Li, G., Chen, J., Huang, Y., An, T., & Zhang, C. (2015). Pollution characteristics and health risk assessment of volatile organic compounds emitted from different plastic solid waste recycling workshops. *Environment International*, *77*, 85–94. https://doi.org/10.1016/j.envint.2015.01.004

Hleis, D., Fernandez-Olmo, I., Ledoux, F., Kfoury, A., Courcot, L., Desmonts, T., & Courcot, D. (2013). Chemical profile identification of fugitive and confined particle emissions from an integrated iron and steelmaking plant. *Journal of Hazardous Materials*, *250-251*, 246–255. https://doi.org/10.1016/j.jhazmat.2013.01.080

Hossaini, R., Atlas, E., Dhomse, S. S., Chipperfield, M. P., Bernath, P. F., Fernando, A. M., et al. (2019). Recent trends in stratospheric chlorine from very short-lived substances. *Journal of Geophysical Research: Atmospheres*, *124*, 2318–2335. https://doi.org/10.1029/2018JD029400

Hossaini, R., Chipperfield, M. P., Montzka, S. A., Leeson, A. A., Dhomse, S. S., & Pyle, J. A. (2017). The increasing threat to stratospheric ozone from dichloromethane. *Nature Communications*, *8*, 15962. https://doi.org/10.1038/ncomms15962

Hossaini, R., Chipperfield, M. P., Saiz-Lopez, A., Harrison, J. J., von Glasow, R., Sommariva, R., et al. (2015). Growth in stratospheric chlorine from short-lived chemicals not controlled by the Montreal Protocol. *Geophysical Research Letters*, *42*, 4573–4580. https://doi.org/10.1002/2015GL063783

Jia, J., Cheng, S., Yao, S., Xu, T., Zhang, T., Ma, Y., et al. (2018). Emission characteristics and chemical components of size-segregated particulate matter in iron and steel industry. *Atmospheric Environment*, *182*, 115–127. https://doi.org/10.1016/j.atmosenv.2018.03.051

Keene, W. C., Khalil, M. A. K., Erickson, D. J., McCulloch, A., Graedel, T. E., Lobert, J. M., et al. (1999). Composite global emissions of reactive chlorine from anthropogenic and natural sources: Reactive Chlorine Emissions Inventory. *Journal of Geophysical Research*, *104*(D7), 8429–8440. https://doi.org/10.1029/1998jd100084

Lee, B. H., Lopez-Hilfiker, F. D., Schroder, J. C., Campuzano-Jost, P., Jimenez, J. L., McDuffie, E. E., et al. (2018). Airborne observations of reactive inorganic chlorine and bromine species in the exhaust of coal-fired power plants. *Journal of Geophysical Research: Atmospheres*, *123*, 11,225–11,237. https://doi.org/10.1029/2018JD029284

Leedham Elvidge, E. C., Oram, D. E., Laube, J. C., Baker, A. K., Montzka, S. A., Humphrey, S., et al. (2015). Increasing concentrations of dichloromethane, CH_2Cl_2, inferred from CARIBIC air samples collected 1998–2012. *Atmospheric Chemistry and Physics*, *15*(4), 1939–1958. https://doi.org/10.5194/acp-15-1939-2015

Liang, Y., Li, Q., Ding, X., Wu, D., Wang, F., Otsuki, T., et al. (2020). Forward ultra-low emission for power plants via wet electrostatic precipitators and newly developed demisters: Filterable and condensable particulate matters. *Atmospheric Environment*, *225*, 117372. https://doi.org/10.1016/j.atmosenv.2020.11737

Liao, J., Huey, L. G., Liu, Z., Tanner, D. J., Cantrell, C. A., Orlando, J. J., et al. (2014). High levels of molecular chlorine in the Arctic atmosphere. *Nature Geoscience*, *7*(2), 91–94. https://doi.org/10.1038/ngeo2046

Liu, X., Qu, H., Huey, L. G., Wang, Y., Sjostedt, S., Zeng, L., et al. (2017). High levels of daytime molecular chlorine and nitryl chloride at a rural site on the North China Plain. *Environmental Science & Technology*, *51*(17), 9588–9595. https://doi.org/10.1021/acs.est.7b03039

McCulloch, A., Aucott, M. L., Benkovitz, C. M., Graedel, T. E., Kleiman, G., Midgley, P. M., & Li, Y.-F. (1999). Global emissions of hydrogen chloride and chloromethane from coal combustion, incineration and industrial activities: Reactive Chlorine Emissions Inventory. *Journal of Geophysical Research*, *104*(D7), 8391–8403. https://doi.org/10.1029/1999jd900025

MEP (2014). The list of running desulfurization facilities for sinter plant at iron and steel manufactory in China, Beijing, China: Ministry of Environmental Protection of the People's Republic of China (MEP). Retrieved from http://www.mee.gov.cn/gkml/hbb/bgg/201407/W020140711581927459581.pdf (in Chinese)

MEP (2016). Environmental annual bulletin of China in 2015. Beijing, China: Ministry of Environmental Protection of the People's Republic of China (MEP). Retrieved from http://www.mee.gov.cn/hjzl/sthjzk/zghjzkgb/201606/P020160602333160471955.pdf (in Chinese)

Mo, Z., Shao, M., Lu, S., Qu, H., Zhou, M., Sun, J., & Gou, B. (2015). Process-specific emission characteristics of volatile organic compounds (VOCs) from petrochemical facilities in the Yangtze River Delta, China. *Science of the Total Environment*, *533*, 422–431. https://doi.org/10.1016/j.scitotenv.2015.06.089

Qiu, X., Ying, Q., Wang, S., Duan, L., Wang, Y., Lu, K., et al. (2019). Significant impact of heterogeneous reactions of reactive chlorine species on summertime atmospheric ozone and free-radical formation in north China. *The Science of the Total Environment*, *693*, 133580. https://doi.org/10.1016/j.scitotenv.2019.133580

Qiu, X., Ying, Q., Wang, S., Duan, L., Zhao, J., Xing, J., et al. (2019). Modeling the impact of heterogeneous reactions of chlorine on summertime nitrate formation in Beijing, China. *Atmospheric Chemistry and Physics*, *19*(10), 6737–6747. https://doi.org/10.5194/acp-19-6737-2019

Rhew, R. C., Teh, Y. A., Abel, T., Atwood, A., & Mazéas, O. (2008). Chloroform emissions from the Alaskan Arctic tundra. *Geophysical Research Letters*, *35*, L21811. https://doi.org/10.1029/2008gl035762

Saiz-Lopez, A., & Glasow, R. (2012). Reactive halogen chemistry in the troposphere. *Chemical Society Reviews*, *41*(19), 6448–6472. https://doi.org/10.1039/c2cs35208g

Shen, L., Xiang, P., Liang, S., Chen, W., Wang, M., Lu, S., & Wang, Z. (2018). Sources profiles of volatile organic compounds (VOCs) measured in a typical industrial process in Wuhan, Central China. *Atmosphere*, *9*, 297. https://doi.org/10.3390/atmos9080297

Shi, J., Deng, H., Bai, Z., Kong, S., Wang, X., Hao, J., et al. (2015). Emission and profile characteristic of volatile organic compounds emitted from coke production, iron smelt, heating station and power plant in Liaoning Province, China. *Science of the Total Environment*, *515-516*, 101–108. https://doi.org/10.1016/j.scitotenv.2015.02.034

Simpson, W. R., Brown, S. S., Saiz-Lopez, A., Thornton, J. A., & Glasow, R. (2015). Tropospheric halogen chemistry: Sources, cycling, and impacts. *Chemical Reviews*, *115*(10), 4035–4062. https://doi.org/10.1021/cr5006638

Simmonds, P. G., Manning, A. J., Cunnold, D. M., McCulloch, A., O'Doherty, S., Derwent, R. G., et al. (2006). Global trends, seasonal cycles, and European emissions of dichloromethane, trichloroethene, and tetrachloroethene from the AGAGE observations at Mace Head, Ireland, and Cape Grim, Tasmania. *Journal of Geophysical Research*, *111*(D18), https://doi.org/10.1029/2006jd007082

Tan, Z., Fuchs, H., Lu, K., Hofzumahaus, A., Bohn, B., Broch, S., et al. (2017). Radical chemistry at a rural site (Wangdu) in the North China Plain: Observation and model calculations of OH, HO_2 and RO_2 radicals. *Atmospheric Chemistry and Physics*, *17*(1), 663–690. https://doi.org/10.5194/acp-17-663-2017

Tang, L., Qu, J., Mi, Z., Bo, X., Chang, X., Anadon, L. D., et al. (2019). Substantial emission reductions from Chinese power plants after the introduction of ultra-low emissions standards. *Nature Energy*, *4*(11), 929–938. https://doi.org/10.1038/s41560-019-0468-1

Tham, Y. J., Wang, Z., Li, Q., Yun, H., Wang, W., Wang, X., et al. (2016). Significant concentrations of nitryl chloride sustained in the morning: Investigations of the causes and impacts on ozone production in a polluted region of northern China. *Atmospheric Chemistry and Physics*, *16*(23), 14,959–14,977. https://doi.org/10.5194/acp-16-14959-2016

Thornton, J. A., Kercher, J. P., Riedel, T. P., Wagner, N. L., Cozic, J., Holloway, J. S., et al. (2010). A large atomic chlorine source inferred from mid-continental reactive nitrogen chemistry. *Nature*, *464*(7286), 271–274. https://doi.org/10.1038/nature08905

Tsai, J. H., Lin, K. H., Chen, C. Y., Lai, N., Ma, S. Y., & Chiang, H. L. (2008). Volatile organic compound constituents from an integrated iron and steel facility. *Journal of Hazardous Materials*, *157*(2–3), 569–578. https://doi.org/10.1016/j.jhazmat.2008.01.022

Wang, H., Nie, L., Li, J., Wang, Y., Wang, G., Wang, J., & Hao, Z. (2013). Characterization and assessment of volatile organic compounds (VOCs) emissions from typical industries. *Chinese Science Bulletin*, *58*(7), 724–730. https://doi.org/10.1007/s11434-012-5345-2

Wang, M., Li, Q., Liu, W., Fang, M., & Han, Y. (2018). Monochlorinated to octachlorinated polychlorinated dibenzo-*p*-dioxin and dibenzofuran emissions in sintering fly ash from multiple-field electrostatic precipitators. *Environmental Science & Technology*, *52*(4), 1871–1879. https://doi.org/10.1021/acs.est.7b04848

Wang, X., Lei, Y., Yan, L., Liu, T., Zhang, Q., & He, K. (2019). A unit-based emission inventory of SO_2, NO_x and PM for the Chinese iron and steel industry from 2010 to 2015. *The Science of the Total Environment*, *676*, 18–30. https://doi.org/10.1016/j.scitotenv.2019.04.241

Wei, W., Wang, S., Chatani, S., Klimont, Z., Cofala, J., & Hao, J. (2008). Emission and speciation of non-methane volatile organic compounds from anthropogenic sources in China. *Atmospheric Environment*, *42*(20), 4976–4988. https://doi.org/10.1016/j.atmosenv.2008.02.044

Wu, Q., Gao, W., Wang, S., & Hao, J. (2017). Updated atmospheric speciated mercury emissions from iron and steel production in China during 2000–2015. *Atmospheric Chemistry and Physics*, *17*(17), 10,423–10,433. https://doi.org/10.5194/acp-17-10423-2017

Yang, H.-H., Lee, K.-T., Hsieh, Y.-S., Luo, S.-W., & Huang, R.-J. (2015). Emission characteristics and chemical compositions of both filterable and condensable fine particulate from steel plants. *Aerosol and Air Quality Research*, *15*(4), 1672–1680. https://doi.org/10.4209/aaqr.2015.06.0398

Zheng, J., Yu, Y., Mo, Z., Zhang, Z., Wang, X., Yin, S., et al. (2013). Industrial sector-based volatile organic compound (VOC) source profiles measured in manufacturing facilities in the Pearl River Delta, China. *Science of the Total Environment*, *456-457*, 127–136. https://doi.org/10.1016/j.scitotenv.2013.03.055